Ben-Israel, M., Matmon, A., Haviv, I., Niedermann, S. (2018): Applying stable cosmogenic 21 Ne to understand surface processes in deep geological time (10 7 –10 8 yr). - *Earth and Planetary Science Letters*, *498*, pp. 266—274.

DOI: http://doi.org/10.1016/j.epsl.2018.07.002

Applying stable cosmogenic ^{21}Ne to understand surface processes in deep geological time (10^7-10^8 yr)

Michal Ben-Israel[1*], Ari Matmon[1], Itai Haviv[2] and Samuel Niedermann[3]

[1]*The Institute of Earth Sciences, Hebrew University of Jerusalem, Jerusalem 91904, Israel*

[2]*Department of Geological and Environmental Sciences, Ben Gurion University, Beer Sheva 84105, Israel*

[3]*Deutsches GeoForschungsZentrum GFZ, Telegrafenberg, D-14473 Potsdam, Germany*

*Corresponding author. Email: michal.benisrael@mail.huji.ac.il

ABSTRACT

This work sets out to test the applicability of stable cosmogenic ^{21}Ne for quantifying the rates of surface processes over time scales of 10^7-10^8 years and the potential limitations and pitfalls associated with such time spans. First, we examine several processes in addition to in-situ production during exposure that affect the final measured concentration of ^{21}Ne. We calculate the magnitude of ^{21}Ne produced by interaction with secondary cosmic ray particles after burial (muogenic Ne) and by non-cosmogenic sources (nucleogenic Ne). We also evaluate the fraction of ^{21}Ne lost through diffusion out of the quartz crystal as a function of time and temperature (depth). We then apply our calculations to ^{21}Ne concentrations measured in sediments that were deposited along the northern passive margin of Gondwana during the late Precambrian, Cambrian, and Lower Cretaceous. In light of the measured concentrations in the sediment samples, we discuss the limitations imposed by our calculations and show that ^{21}Ne concentrations measured in Lower Cretaceous samples can be interpreted in terms of surface

exposure times or average erosion rates during the time of erosion and transport. In contrast, concentrations measured in Cambrian and Precambrian samples are limited in their use as surface process indicators although they still yield valuable geological information. We conclude that this novel application of in situ stable cosmogenic nuclides holds the potential as a tool for quantifying surface processes and understanding landscape evolution during the deep geological past and provides insight into macro-scale processes that have shaped Earth over the past hundreds of millions of years.

1. INTRODUCTION

The most commonly used *in-situ* stable cosmogenic nuclides in the study of surface processes are the noble gas isotopes ^{3}He and ^{21}Ne. Cosmogenic ^{21}Ne in quartz is produced mainly from neutron spallation through the reaction ^{28}Si(n,2α)^{21}Ne (Dunai, 2010; Gosse and Phillips, 2001; Niedermann, 2002). Noble gas isotopes are a useful tool in quantitative geomorphology due to the fact that they are highly incompatible elements with low geological background concentrations (Dunai, 2010). Furthermore, stable nuclides record cosmic ray irradiation for a potentially infinite length of time, meaning it is possible to investigate exposure histories significantly longer than those imposed by the half-life of radiogenic nuclides (Niedermann, 2002).

The quantitative retention of cosmogenic ^{21}Ne in quartz over geologic time at Earth surface temperatures has been verified by consistent ages of exposure calculated from ^{10}Be, ^{26}Al, and ^{21}Ne (Hetzel et al., 2002; Kober et al., 2011). In this study, we focus on ^{21}Ne in quartz and test the applicability and limitations of using it for quantifying the rates of surface processes over time scales of 10^{7}-10^{8} years. We apply our results to ^{21}Ne concentrations measured in sediments

deposited along the northern passive margin of Gondwana during the late Precambrian, Cambrian, and Lower Cretaceous and conclude that the ^{21}Ne signal in the Lower Cretaceous samples (~140 Ma) can be interpreted in terms of paleo surface exposure ages and erosion rates. In contrast, the use of ^{21}Ne in the Cambrian and Precambrian samples is limited as a tool for quantifying paleo rates. However, combined with independent geological evidence, still could yield valuable information.

2. LIMITATIONS IN EVALUATING *IN SITU* PRODUCED COSMOGENIC ^{21}Ne

To utilize ^{21}Ne in the study of surface processes, we must determine the amount of cosmogenic ^{21}Ne produced during exposure. Several processes other than in situ production during exposure affect the total ^{21}Ne concentration measured in quartz: 1) trapped ^{21}Ne from atmospheric, mantle, or crustal sources, 2) post-burial production of cosmogenic ^{21}Ne by muons, 3) non-cosmogenic (nucleogenic) ^{21}Ne produced in the quartz lattice, and 4) ^{21}Ne diffusion out of the quartz lattice.

The total ^{21}Ne concentration measured in each sample is, therefore, the sum of several components:

$$^{21}Ne_{measured} = {}^{21}Ne_{surface} + {}^{21}Ne_{post\text{-}burial} + {}^{21}Ne_{trapped} + {}^{21}Ne_{nucleogenic} - {}^{21}Ne_{diffused} \quad (1)$$

where $^{21}Ne_{surface}$ is the cosmogenic ^{21}Ne produced by neutrons at or near the surface during sediment exposure. $^{21}Ne_{surface}$ is the value of interest as it can be used to calculate rates of surface processes. $^{21}Ne_{post\text{-}burial}$ is a cosmogenic component produced at depth by muons after the sediment's burial and so cannot record rates of surface processes. $^{21}Ne_{trapped}$ is the non-cosmogenic trapped atmospheric, mantle, or crustal ^{21}Ne residing in the crystal lattice or

inclusions. $^{21}Ne_{nucleogenic}$ is the non-cosmogenic ^{21}Ne produced within the crystal lattice by natural nuclear reactions related to U and Th decay. Lastly, $^{21}Ne_{diffused}$ is the fraction of Ne diffused out of the crystal.

We follow the ^{21}Ne evaluation scheme suggested by Niedermann (2002), using an approximation for cosmogenic ^{21}Ne determined after subtracting of $^{21}Ne_{trapped}$ and $^{21}Ne_{nucleogenic}$ from the total measured ^{21}Ne. We present here additional calculations and modifications to this scheme for extremely old samples. Such cases, where $^{21}Ne_{surface}$ is observed (or expected) to be similar or smaller compared to ^{21}Ne from other components, must withstand rigorous scrutiny.

2.1 Trapped ^{21}Ne

Trapped Ne ($Ne_{trapped}$) originates from crustal, mantle or atmospheric sources, incorporated in the crystal lattice or fluid inclusions during crystallization or metamorphism (Farley and Poreda, 1993; Kennedy et al., 1990). To minimize the interferences of such Ne, the quartz grains selected for analysis should contain little to no visible inclusions. To further reduce the trapped Ne concentration, quartz grains are crushed to <~100µm grain size before stepwise heating. The $^{21}Ne_{trapped}$ component that cannot be avoided through sample selection and preparation must be corrected for. This is done by subtracting the $Ne_{trapped}$ component from the measured composition of Ne. In cases where the $Ne_{trapped}$ composition is significantly different from atmospheric, it can be determined by mechanical crushing in vacuum of aliquots from the same or representative samples (e.g., Hetzel et al., 2002). Since only a fraction of the trapped Ne is released during crushing, the sum of the non-trapped components (the excess ^{21}Ne, abbreviated as $^{21}Ne_{ex}$) is determined by the subtraction of the $(^{21}Ne/^{20}Ne)_{trapped}$ ratio from the $^{21}Ne/^{20}Ne$ ratio determined during stepwise heating (Niedermann, 2002; see section 2.3):

$^{21}Ne_{ex} = (^{21}Ne/^{20}Ne_{heating} - ^{21}Ne/^{20}Ne_{trapped}) * ^{20}Ne_{heating}$ (2).

2.2 Cosmogenic ^{21}Ne produced at the surface ($^{21}Ne_{surface}$) and at depth ($^{21}Ne_{post\text{-}burial}$)

Both $^{21}Ne_{surface}$ and $^{21}Ne_{post\text{-}burial}$ are two cosmogenic components produced in situ within the quartz grain and therefore cannot be distinguished analytically (however, the post-burial component could be corrected for by using depth profile measurements as it changes with depth unlike $^{21}Ne_{surface}$). We present the following evaluations for muogenic ^{21}Ne production in quartz over extended periods, to achieve as accurate an approximation as possible so that $^{21}Ne_{post\text{-}burial}$ can be calculated and corrected for.

The near-surface contribution of ^{21}Ne production by fast muon interactions and negative muon capture may account for up to ~3.6% of the total production rate at sea level and high latitudes (SLHL; Balco and Shuster, 2009). As depth increases, the relative contribution of ^{21}Ne production by muons also increases until fast muon interactions become the major pathway for ^{21}Ne production. Therefore, the contribution of fast muon interactions at depth can be significant when integrated over long periods of time. Ignoring this contribution may lead to overestimation of sediment exposure ages or underestimation of erosion rates. Unlike fast muons, it is unclear whether negative muon capture reactions in Si can produce ^{21}Ne to a significant extent (Heisinger et al., 2002a; Heisinger et al., 2002b; Fernandez-Mosquera et al., 2010). However, following the scheme presented by Heisinger et al. (2002a,b), MATLAB implementation from Balco et al. (2008), and using the calculated probability for particle emission (f^*) presented by Fernandez-Mosquera et al. (2010), we calculate the post-burial muogenic Ne production in quartz integrated over extended periods (complete calculation is available in the supplementary material A1).

We performed calculations for depths up to 1000 meters below the surface, at sea level, and integrated them over periods of $1{\cdot}10^7$ to $1{\cdot}10^9$ years (Fig. 1). ^{21}Ne concentrations $<1{\cdot}10^5$ atoms/g quartz are in the same order of magnitude as the typical uncertainty of cosmogenic ^{21}Ne concentrations measurable in quartz (Niedermann, 2002), and can, therefore, be ignored. We find that production of ^{21}Ne by negative muons over periods of up to $1{\cdot}10^9$ years is too low to be computed at depths exceeding 730 meters and does not exceed $1{\cdot}10^5$ atoms/g quartz at depths greater than 60 meters (Fig. 1b). We consider this a maximum calculation as it is unclear whether such production occurs. Production rates due to higher energy fast muon interactions do not decrease as rapidly with depth. The minimum burial depth below which post-burial production of ^{21}Ne can be considered insignificant ($<1{\cdot}10^5$ atoms/g or smaller) is 920 meters for periods of $1{\cdot}10^9$, 770 meters for $5{\cdot}10^8$, 480 meters for $1{\cdot}10^8$, 380 meters for $5{\cdot}10^7$, and 200 meters for $1{\cdot}10^7$ years. While production by negative muon capture can be ignored below depths of 60 meters, ^{21}Ne produced post-burial in quartz by fast muons should be accounted for quartz grains that have been buried continuously over extended periods. $^{21}Ne_{post\text{-}burial}$ can be minimized by sample collection from sufficient depths and if needed calculated and corrected for.

2.3 Nucleogenic ^{21}Ne

Nucleogenic ^{21}Ne is produced through the α-capture reaction $^{18}O(\alpha,n)^{21}Ne$ (Yatsevich and Honda, 1997). These reactions are triggered by the nuclear decay of U and Th found either in minerals surrounding the quartz or concentrated in inclusions within the crystal lattice (Niedermann, 2002). The contribution of nucleogenic ^{21}Ne may be significant and must be considered, especially when dealing with samples with extensive geological histories.

In quartz, ^{21}Ne is often measured over several temperature steps, such as 400, 600, 800, and 1200°C, allowing for a more accurate discrimination between the cosmogenic and non-cosmogenic Ne components, based on their distinct $^{21}Ne/^{20}Ne$ and $^{22}Ne/^{20}Ne$ ratios (Niedermann, 2002). If quartz grains have been crushed to ~100 µm grain size or smaller prior to stepwise heating, nearly all of the cosmogenic ^{21}Ne is released in the ≤800°C heating steps (Niedermann, 2002). The ^{21}Ne released in the higher temperature steps consists essentially of $Ne_{trapped}$ and the nucleogenic Ne remaining after careful sample selection and preparation ($Ne_{nucleogenic}$).

Further understanding of the different components of Ne can be extracted using Ne three-isotope systematics, where the three stable isotopes of Ne are plotted as $^{21}Ne/^{20}Ne$ versus $^{22}Ne/^{20}Ne$ (Niedermann, 2002; Niedermann et al., 1993). The three-isotope plot presents the signatures of Ne components and their mixing lines. Cosmogenic Ne will fall on a mixing line between atmospheric Ne (or some other kind of trapped Ne) and the cosmogenic end member – the spallation line. Enrichment of nucleogenic ^{21}Ne will cause a horizontal shift, while nucleogenic ^{22}Ne (produced by the reaction $^{19}F(\alpha,n)^{22}Na(\beta^+)^{22}Ne$), if present, would cause a vertical shift. To some extent, deviations from the spallation line can also be the result of isotopic mass fractionation processes (Niedermann et al., 1994).

In cases where nucleogenic ^{21}Ne accounts for a significant component of the total ^{21}Ne measured in quartz samples, we suggest computing the nucleogenic ^{21}Ne formed within the crystal. The total nucleogenic Ne produced in quartz can be calculated using the measured U and Th concentrations (Yatsevich and Honda, 1997). We approximated the nucleogenic ^{21}Ne contribution using the (U–Th)/Ne system based on Gautheron et al. (2006):

$$^{21}\text{Ne} = 2.59 \cdot 10^{9} \cdot [U]((8 \cdot 4.04 \cdot 10^{-8}(e^{\lambda_{238U} \cdot t} - 1)) + (7 \cdot 7.20 \cdot 10^{-3} \cdot 5.62 \cdot 10^{-8} \cdot (e^{\lambda_{235U} \cdot t} - 1)) + (6 \cdot 6.08 \cdot 10^{-8} \cdot (e^{\lambda_{232Th} \cdot t} - 1) \cdot \frac{[Th]}{[U]})) \quad (3)$$

where λ_i are the decay constants, t is the duration of production, U and Th concentrations are in ppm and ^{21}Ne is in 10^6 atoms. The amount of nucleogenic ^{21}Ne produced in quartz grains has been calculated for U and Th concentrations ranging between 0 and 2 ppm, which are close to the ranges for measured samples. Ejection or implantation corrections were not performed as the outer rims of the grains were removed by chemical etching. The production rate factors for each decay chain in eq. 3 were taken from Cox et al. (2015). Nucleogenic ^{21}Ne produced in quartz over $1.4 \cdot 10^8$, $4.2 \cdot 10^8$, and $6 \cdot 10^8$ years (the age of the oldest samples) varies between 0 and ~$230 \cdot 10^6$ atoms/g quartz (Fig. 2). It is important to note that this calculation represents the maximal nucleogenic ^{21}Ne concentrations produced as it does not take into account the $^{21}Ne_{nucleogenic}$ lost by diffusion (see 2.4).

2.4 Diffusion of Ne from the quartz lattice

The quantitative retention of cosmogenic Ne in quartz over geologic time at Earth surface temperatures has been verified by comparing ages of exposure calculated from ^{10}Be, ^{26}Al, and ^{21}Ne (e.g., Hetzel et al., 2002; Niedermann, 2002). Thermally activated diffusion from quartz grains is dependent on time and grain radius (Shuster and Farley, 2005). Previous work on noble gas diffusion in quartz revealed a linear Arrhenius diffusion curve at low-temperatures (<200°C). Ne diffusion displays a linear behavior (Tremblay et al., 2014a) and can, therefore, be modeled using given kinetic parameters (Shuster and Farley, 2005). When considering burial over

geological timescales at depths of 1-2 km, where temperatures increase to 50°C and more, underestimation of the real exposure age due to diffusion presents a considerable concern.

We calculated the fractional loss of Ne over time for grain diameters of 100, 250, 400, and 850µm at temperatures of 40, 50 and 60°C, using the equations of Fechtig and Kalbitzer (1966) and diffusion kinetic coefficients presented by Tremblay et al. (2014a):

$$D = D_0 e^{\frac{-E_a}{R \cdot T}} \quad (4)$$

where E_a is the activation energy (ranging from 95.7 to 153.8 kJ/mol), D_0 is the Frequency Factor (ranging from $6.6 \cdot 10^{-5}$ to $3.2 \cdot 10^{-1}$ m^2/s), T is the temperature in K and R is the gas constant. Our calculations of fractional loss of Ne at constant temperatures of 40, 50 and 60°C correspond to a geothermal gradient of 20 K/km, a temperature of 20°C at the surface and depths of 1000, 1500 and 2000m and were performed over a time range of 0-600 Myr of constant burial (Fig. 3). For the maximal burial period of 600 Myr, the fractional Ne loss is 19-95% at 40°C (a), 44-100% at 50°C (b), and 82-100% at 60°C (c), depending on grain size (100-850µm).

Loss of Ne through diffusion over extended periods can lead to underestimating the correct surface age. Correcting for diffusion is theoretically possible using the sample's grain size distribution and burial depth. However, while grain size distribution can be measured and accounted for, the thermal history of quartz grains depends on the regional thermal history, which is controlled by regional tectonic activity, heating events triggered by magmatic and hydrothermal processes, and of course the burial depth of the sample which is subject to changes with loading/unloading at the sampling site. It is therefore extremely difficult to accurately correct for the Ne lost by diffusion, especially when considering samples of pre-Mesozoic age. In order to

191 best approximate the effect of Ne diffusion from the quartz grains, sampling sites must be
192 carefully selected, taking into account the geological history of the area.

193 3. TESTING APPLICABILITY FOR NATURAL SAMPLES

194 In light of the theoretical modeling presented above, we test the applicability of cosmogenic in
195 situ produced ^{21}Ne as an indicator for surface process characteristics on three sets of samples:
196 Precambrian, Cambrian, and Lower Cretaceous sandstones. We present an approximation for in
197 situ cosmogenic ^{21}Ne produced during transport and exposure of the investigated sediments and
198 evaluate the effect of the various production paths of Ne on this approximation. We then discuss
199 whether the samples presented can be used to interpret in terms of surface residence time or
200 erosion rates.

201 3.1 Geological background

202 In the late Neoproterozoic (~600Ma), the Pan-African orogenic cycle that amalgamated east and
203 west Gondwana abated. Throughout most of the Phanerozoic, cratonic conditions prevailed
204 along the northern passive margin of Gondwana, punctuated by several episodes of epeirogenic
205 vertical movements, between which sedimentation occurred (Garfunkel, 1999). The sedimentary
206 cover includes a thick sequence of quartz-rich sediments that extend from Morocco in the west
207 to Jordan in the east (Avigad et al., 2003). This relative tectonic stability was only interrupted in
208 the mid-Cenozoic (~20Ma) by continental breakup of the Arabo-African continent and rifting of
209 the Red Sea and Suez (Garfunkel, 1980). During the ~550 million years of tectonic stability in the
210 area, the mature platformal sediment cover was never thick enough to trigger metamorphism.
211 These unique conditions allowed for the burial of sediments at optimum depths, shallow enough,

where no significant heating occurred, with respect to ^{21}Ne retention in quartz, and deep enough for post-burial production to be minimal.

3.2 Sample collection and preparation for analytical procedure

To assure that the cosmogenic ^{21}Ne measured was produced during the sediment's original exposure, we collected sediment samples from boreholes drilled across Israel (Fig. 4). This depth range ensures that samples have been buried continuously at optimum depths. A total of 10 samples are presented in this study (Table 1). Four samples of late Precambrian age were collected from the Sinaf1 and Ramon1 boreholes (Fig. 4, Table 1). Three samples of Cambrian age were collected from the Sinaf1 borehole (Fig. 4, Table 1). Three samples of Lower Cretaceous age were collected from the Sinaf1, Jericho1 Deep, and Ramim Ridge boreholes (Fig. 4, Table 1).

Samples were processed to separate clean quartz at the Institute of Earth Sciences Cosmogenic Isotope Laboratory, Hebrew University of Jerusalem, Israel, following standard procedures (Kohl and Nishiizumi, 1992; Hetzel et al., 2002). The samples were first leached in HCl/HNO_3 mixture (3:1) at a temperature of 150°C for 1.5h dissolving carbonates and iron oxides. This procedure was followed by magnetic separation to isolate quartz further. Samples were then treated by a series of three leachings in 1% HF/HNO_3 mixture for 7, 12 and 24h at 70°C, removing the outer rims of the quartz grains.

He and Ne concentrations and isotopic ratios were determined in the 63-250µm size fraction (crushed to ~100 µm maximum before loading) at the noble gas laboratory at GFZ Potsdam, Germany, following procedures described in Niedermann et al. (1997). Gas extraction was accomplished by stepwise heating at 400, 600, 800 and 1,200°C. The isotopic composition of

trapped Ne was determined by mechanical crushing in vacuum of aliquots from representative samples.

3.3 Determining $^{21}Ne_{surface}$ in natural samples

Considering the $Ne_{postburial}$ fraction of the cosmogenic Ne, all depths presented are greater than 260 meters (Table 1), and thus the contribution by post-burial production is similar to the analytical uncertainties or smaller and was therefore ignored (Fig. 1). Consequently, and by following Niedermann's (2002) scheme, the $^{21}Ne_{ex}$, calculated compared to the crushed aliquot isotopic composition, of the 400-800°C steps approximate $^{21}Ne_{surface}$ if nucleogenic Ne can be neglected or accounted for in these steps.

In the Precambrian and Cambrian samples, comparison of the combined $^{21}Ne_{ex}$ measured in the 400-800°C steps with that measured in the 1200°C step, where no cosmogenic Ne is expected (Niedermann, 2002), shows that the latter are similar and often even higher (Fig. 5a). The $^{21}Ne_{ex}$ in the 1200°C step is accompanied by a corresponding excess in ^{22}Ne and must be interpreted as nucleogenic Ne. Because of the large contribution of that component, the question arises whether the $^{21}Ne_{ex}$ measured in the 400-800°C steps is indeed purely cosmogenic or whether it includes a significant contribution of nucleogenic Ne as well. The three-isotope plots are not conclusive in that respect, as most 400-800°C data plot below the spallation line (Niedermann et al., 1993) and close to the atmospheric composition (as shown in the supplementary materials A3, Figs. S1-S8), indicating a substantial isotope fractionation effect superimposed on a multi-component mixture of trapped Ne, cosmogenic Ne, and perhaps several different kinds of nucleogenic Ne. Lower Cretaceous samples CSN2 and CRR1 present slightly higher concentrations of $^{21}Ne_{ex}$ in the 400-800°C compared to that measured in the 1200°C step (Fig. 5a). Yet in contrast

to the Precambrian and Cambrian samples, the $^{21}Ne/^{20}Ne$ and $^{22}Ne/^{20}Ne$ ratios fall within error on the spallation line (Figs. S1-S8), suggesting that the $^{21}Ne_{ex}$ measured in the 400-800°C steps is more likely to be cosmogenic.

To help evaluate the maximal nucleogenic ^{21}Ne contribution, we calculated its expected production using the U and Th concentrations measured in the clean quartz samples and the duration of burial of the samples (580, 430 and 130 Ma for the Precambrian, Cambrian and Lower Cretaceous samples, respectively; Table 3). The age of sedimentation represents the known age under which the quartz has experienced thermal stability. While this might cause an underestimation of $Ne_{nucleogenic}$, the history of the quartz grains prior to deposition is unknown, and may have included periods of heating (i.e.: during exhumation from bedrock, due to periods of burial, and by hydrothermal activity). Therefore, this calculation, while not exact, is a reasonable estimation of $Ne_{nucleogenic}$.

We assumed the $^{21}Ne_{ex}$ in the 1200°C stage to essentially correspond to total nucleogenic ^{21}Ne measured. This is a reasonable approximation, though it might be an underestimate of nucleogenic ^{21}Ne (Niedermann et al., 1994). A comparison between the calculated and measured nucleogenic ^{21}Ne shows, as expected, considerably lower concentrations of measured nucleogenic ^{21}Ne, caused by Ne loss due to diffusion from the quartz grains during burial (Fig. 5b).

If we assume that the $^{21}Ne_{ex}$ measured in the 1200°C step represents most of the nucleogenic ^{21}Ne released in the heating steps (this assumption is justified as $^{21}Ne_{ex}$(1200°C) is >40% of the total $^{21}Ne_{ex}$ released), we can further propose that measured nucleogenic ^{21}Ne to calculated

276 nucleogenic ^{21}Ne represents the fraction of ^{21}Ne retained after diffusion. If so, this ratio is valid
277 for both the nucleogenic and the cosmogenic components. Comparing the ^{21}Ne loss calculated
278 directly by the diffusion equation (eq. 4) to the fraction of nucleogenic ^{21}Ne retained (indicated
279 by the ratio of measured to calculated nucleogenic Ne), we can see that in most cases the two
280 calculations agree within error (Table 3). The Lower Cretaceous sample from the Jericho1
281 borehole (CJR1) is the only one showing significantly higher calculated diffusion compared to
282 nucleogenic Ne retention (for the <250µm grain size measured). This observation is not easily
283 explained, but it is possible that the diffusion calculation is an overestimate. Previous work on
284 noble gas diffusion shows variability in diffusion kinetics for different quartz samples (Tremblay
285 et al., 2014b). Furthermore, it has been suggested that radiation damage and inclusions in the
286 crystal increase overall noble gas retentivity in a solid material and may affect some crystals
287 (Shuster and Farley, 2005).

288 The overall calculated ^{21}Ne loss by diffusion depends on temperature (burial depth) and grain
289 size, both of which are approximated values. In the Precambrian and Cambrian samples, the
290 evaluated overall ^{21}Ne diffused out of the quartz for a grain size of 250µm is significant (~100%
291 in the Precambrian samples and 42-49% in the Cambrian samples). Such a significant loss makes
292 it hard to correct for. However, Ne loss in the Lower Cretaceous samples is considerably lower.
293 In samples CSN2 and CRR1, diffusion for a grain size of 250µm is below 23% and might even be
294 as low as 12% in CRR1. Due to its burial depth (1441 m), the calculated ^{21}Ne loss by diffusion in
295 sample CJR1 is close to 80% (Table 3, Fig. 5b). We can see here that for sediments buried for ~130
296 Myr, at burial depths shallower than 1000m, ^{21}Ne loss due to diffusion, while not negligible, could
297 be corrected. Combining the diffusion with nucleogenic Ne retention, a relatively good correction

298 can be made for $^{21}Ne_{surface}$, given that the sediments did not lose the majority of their original
299 ^{21}Ne.

300 If we consider the 400-800°C $^{21}Ne_{ex}$ of the Lower Cretaceous samples CSN2 and CRR1 to be
301 cosmogenic, we can make a first-order evaluation of exposure ages at or near the surface of these
302 samples using a known production rate of ^{21}Ne. We can correct the 400-800°C $^{21}Ne_{ex}$ measured
303 in these samples based on diffusional loss calculated for 250µm grain and the nucleogenic Ne
304 retention and get a range of 3.3-4.2·10^6 atoms/g quartz for CRR1 and 9.1-10.4·10^6 atoms/g quartz
305 for CSN2. Given a known latitude and elevation, we can translate these values into sediment
306 transport rates to get a better understanding of this paleo-river. However, when we consider the
307 $Ne_{surface}$ concentration deduced we must take into consideration that the cosmogenic ^{21}Ne
308 measured may not only represent the cosmogenic ^{21}Ne produced during Lower Cretaceous
309 exposure and transport but also the inherited cosmogenic ^{21}Ne produced during previous
310 sedimentary cycles. Therefore, for us to make such suppositions we need additional sampling
311 and data analysis that is beyond the scope of this current work.

312 **4. CONCLUSIONS AND SUMMARY**

313 The results presented raise the question whether we can consider *in situ* stable cosmogenic ^{21}Ne
314 measured in extremely old sediments as a tool to understand rates of surface processes in the
315 deep geological past. For Precambrian and Cambrian sediments, the simple answer is no. High
316 nucleogenic ^{21}Ne measured in the 1200°C step compared to the 400-800°C steps makes it hard
317 to interpret the 400-800°C $^{21}Ne_{ex}$ as $^{21}Ne_{surface}$. Furthermore, a significant loss of Ne by diffusion
318 as estimated both by nucleogenic Ne retention and diffusion calculations does not allow
319 meaningful correction of $^{21}Ne_{surface}$. However, Lower Cretaceous sediments show a great promise

for surface process calculations. $^{21}Ne_{ex}$ measured in the 400-800°C steps can be interpreted as $^{21}Ne_{surface}$, and for the two samples buried above 1000m depth, we can rule out the complete loss of Ne due to diffusion. The relatively young age of these sediments (~130 Myr) is still significantly older than the oldest samples analyzed so far for studies of surface processes using cosmogenic nuclides (28 Myr; Libarkin et al., 2002), opening a large window of opportunities for paleo-geomorphological research.

We described here the pitfalls, solutions, and limitations of using stable cosmogenic *in situ* ^{21}Ne to study rates of surface processes in the deep geological past. Even though we could only confidently use a few of the samples for geomorphological study, we suggest that *in situ* cosmogenic ^{21}Ne can be used as a tool to help understand geomorphic processes in the deep geological past (>10^7 yr). We are confident that the tools offered in this work can help expand the present boundaries of this method. Applying this method is not without difficulties. Nonetheless, a better understanding of its limitations allows quantitative understanding of surface processes and identification of different depositional environments. It is crucial for this application (as for many others used in geological research) that it is not implemented without considering the geological context.

ACKNOWLEDGEMENTS

This research is funded by the Israel Science Foundation (ISF grant 385/14 to AM) and was further supported by Minerva Stiftung, DAAD travel grants, and GFZ Potsdam. Many thanks to E.

340 Schnabel, Y. Geller, and O. Tirosh for laboratory assistance. We thank the two anonymous
341 reviewers for the insightful and helpful comments, which significantly improved this manuscript.

342 **APPENDIX A. SUPPLEMENTARY DATA**

343 Supplementary data associated with this article can be found, in the online version, at: xxxx.

344 **REFERENCES**

345 Avigad, D., Kolodner, K., McWilliams, M., Persing, H., Weissbrod, T., 2003. Origin of northern Gondwana
346 Cambrian sandstone revealed by detrital zircon SHRIMP dating. Geology 31, 227–230.
347 doi:10.1130/0091-7613(2003)031<0227:OONGCS>2.0.CO;2

348 Balco, G., Shuster, D.L., 2009. Production rate of cosmogenic 21Ne in quartz estimated from 10Be, 26Al,
349 and 21Ne concentrations in slowly eroding Antarctic bedrock surfaces. Earth Planet. Sci. Lett. 281,
350 48–58. doi:10.1016/j.epsl.2009.02.006

351 Balco, G., Stone, J.O., Lifton, N.A., Dunai, T.J., 2008. A complete and easily accessible means of
352 calculating surface exposure ages or erosion rates from 10Be and 26Al measurements. Quat.
353 Geochronol. 3, 174–195. doi:10.1016/j.quageo.2007.12.001

354 Cox, S.E., Farley, K.A., Cherniak, D.J., 2015. Direct measurement of neon production rates by (α,n)
355 reactions in minerals. Geochim. Cosmochim. Acta 148, 130–144. doi:10.1016/j.gca.2014.08.036

356 Dunai, T.J., 2010. Cosmogenic nuclides: principles, concepts and applications in the earth surface
357 sciences. Cambridge University Press, Cambridge. doi: 10.1017/cbo9780511804519

358 Farley, K.A., Poreda, R.J., 1993. Mantle neon and atmospheric contamination. Earth Planet. Sci. Lett.
359 114, 325–339. doi:10.1016/0012-821X(93)90034-7

360 Fechtig, H., Kalbitzer, S., 1966. The Diffusion of Argon in Potassium-Bearing Solids, in: Potassium Argon
361 Dating. Springer Berlin Heidelberg, Berlin, Heidelberg, pp. 68–107. doi:10.1007/978-3-642-87895-
362 4_4

363 Fernandez-Mosquera, D., Hahm, D., Marti, K., 2010. Calculated rates of cosmic ray muon-produced Ne in
364 subsurface quartz. Geophys. Res. Lett. 37. doi:10.1029/2010GL044106

365 Garfunkel, Z., 1999. History and paleogeography during the Pan-African orogen to stable platform
366 transition: reappraisal of the evidence from the Elat area and the northern. Isr. J. Earth Sci. 48,
367 135–157.

368 Garfunkel, Z., 1980. Contribution to the geology of the Precambrian of the Eilat area. Isr. J. Earth Sci. 29,
369 25–40.

370 Gautheron, C.E., Tassan-Got, L., Farley, K.A., 2006. (U-Th)/Ne chronometry. Earth Planet. Sci. Lett. 243,
371 520–535. doi:10.1016/j.epsl.2006.01.025

372 Gosse, J.C., Phillips, F.M., 2001. Terrestrial in situ cosmogenic nuclides:theory and application. Quat. Sci.

Rev. 20, 1475–1560. doi:10.1016/S0277-3791(00)00171-2

Heisinger, B., Lal, D., Jull, a. J.T., Kubik, P., Ivy-Ochs, S., Knie, K., Nolte, E., 2002a. Production of selected cosmogenic radionuclides by muons: 1. Fast Muons. Earth Planet. Sci. Lett. 200, 357–369. doi:10.1016/S0012-821X(02)00641-6

Heisinger, B., Lal, D., Jull, a. J.T., Kubik, P., Ivy-Ochs, S., Knie, K., Nolte, E., 2002b. Production of selected cosmogenic radionuclides by muons: 2. Capture of negative muons. Earth Planet. Sci. Lett. 200, 357–369. doi:10.1016/S0012-821X(02)00641-6

Hetzel, R., Niedermann, S., Ivy-Ochs, S., Kubik, P.W., Tao, M., Gao, B., 2002. 21Ne versus 10Be and 26Al exposure ages of fluvial terraces: the influence of crustal Ne in quartz. Earth Planet. Sci. Lett. 201, 575–591. doi: 10.1016/S0012-821X(02)00748-3

Kennedy, B.M., Hiyagon, H., Reynolds, J.H., 1990. Crustal neon: a striking uniformity. Earth Planet. Sci. Lett. 98, 277–286. doi: 10.1016/0012-821X(90)90030-2

Kober, F., Alfimov, V., Ivy-Ochs, S., Kubik, P.W., Wieler, R., 2011. The cosmogenic 21Ne production rate in quartz evaluated on a large set of existing 21Ne-10Be data. Earth Planet. Sci. Lett. 302, 163–171. doi:10.1016/j.epsl.2010.12.008

Kohl, C.P., Nishiizumi, K., 1992. Chemical isolation of quartz for measurement of in-situ -produced cosmogenic nuclides. Geochim. Cosmochim. Acta 56, 3583–3587. doi:10.1016/0016-7037(92)90401-4

Libarkin, J.C., Quade, J., Chase, C.G., Poths, J., McIntosh, W., 2002. Measurement of ancient cosmogenic 21Ne in quartz from the 28 Ma Fish Canyon Tuff, Colorado. Chem. Geol. 186, 199–213. doi:10.1016/S0009-2541(01)00411-9

Niedermann, S., 2002. Cosmic-Ray-Produced Noble Gases in Terrestrial Rocks: Dating Tools for Surface Processes. Rev. Mineral. Geochemistry 47, 731–784. doi:10.2138/rmg.2002.47.16

Niedermann, S., Bach, W., Erzinger, J., 1997. Noble gas evidence for a lower mantle component in MORBs from the southern East Pacific Rise: Decoupling of helium and neon isotope systematics. Geochim. Cosmochim. Acta 61, 2697–2715. doi:10.1016/S0016-7037(97)00102-6

Niedermann, S., Graf, T., Kim, J., Kohl, C., 1994. Cosmic-ray-produced 21Ne in terrestrial quartz: the neon inventory of Sierra Nevada quartz separates. Earth Planet. Sci. Lett. 125, 341–355. doi:10.1016/0012-821X(94)90225-9

Niedermann, S., Graf, T., Marti, K., 1993. Mass spectrometric identification of cosmic-ray-produced neon in terrestrial rocks with multiple neon components. Earth Planet. Sci. Lett. 118, 65–73. doi:10.1016/0012-821X(93)90159-7

Shuster, D.L., Farley, K.A., 2005. Diffusion kinetics of proton-induced 21Ne, 3He, and 4He in quartz. Geochim. Cosmochim. Acta 69, 2349–2359. doi:10.1016/j.gca.2004.11.002

Tremblay, M.M., Shuster, D.L., Balco, G., 2014a. Cosmogenic noble gas paleothermometry. Earth Planet. Sci. Lett. 400, 195–205. doi:10.1016/j.epsl.2014.05.040

Tremblay, M.M., Shuster, D.L., Balco, G., 2014b. Diffusion kinetics of 3He and 21Ne in quartz and implications for cosmogenic noble gas paleothermometry. Geochim. Cosmochim. Acta 142, 186–204. doi:10.1016/j.gca.2014.08.010

Yatsevich, I., Honda, M., 1997. Production of nucleogenic neon in the Earth from natural radioactive decay. J. Geophys. Res. 102, 10291–10298. doi:10.1029/97JB00395

Zulauf, G., Romano, S.S., Dörr, W., Fiala, J., 2007. Crete and the Minoan terranes: Age constraints from U-Pb dating of detrital zircons. Geol. Soc. Am. Spec. Pap. 423, 401–411. doi:10.1130/978-0-8137-2423-2

FIGURE CAPTIONS

Figure 1. ^{21}Ne concentration produced by fast (a) and negative (b) muons at depth below surface over time spans of $1{\cdot}10^7$-$5{\cdot}10^8$ years (shown by different colors). As discussed in section 2.2, post-burial production rates of ^{21}Ne are calculated for depths ranging 0-800m and integrated over timespans of 10, 50, 100, 500 Myr, and 1Gyr. For the detailed calculations of muon fluxes and the expected rates of ^{21}Ne production see supplementary materials A2.

Figure 2. Nucleogenic ^{21}Ne produced in quartz crystal lattice over a period of 600 Myr as a function of eU (effective uranium, a parameter that weights the decay of the U and Th parents for their alpha productivity, computed as [U]+0.235·[Th]) and U/Th concentration ratio. Colors indicate U/Th ratios, as shown by the color bar on the right side.

Figure 3. Ne diffusion for different sized quartz grains (shown by different colors) over 600 Myr. Diffusion calculations (see text for details) were performed for constant temperatures of 40, 50 and 60°C and do not account for complex thermal histories.

Figure 4. (a) General location map of the area (marked by a black frame in the inset) and locations of sampling sites used in this study (marked by open circles). The samples were all deposited on the passive northern margin of Gondwana. (b) The modern work area is marked by a black square on a reconstructed map of Gondwana (Zulauf et al., 2007).

Figure 5. (a) $^{21}Ne_{ex}$ extracted in the 400-800°C and 1200°C steps, respectively. $^{21}Ne_{ex}$ concentrations in the 1200°C step are similar or higher than those in the 400-800°C steps, pointing to a considerable nucleogenic ^{21}Ne component. (b) The ratio of $^{21}Ne_{ex}$ released in the 1200°C temperature step (assumed to correspond to measured nucleogenic ^{21}Ne) to calculated nucleogenic ^{21}Ne plotted versus depth. The nucleogenic ^{21}Ne was calculated for 580 Myr of

production for the Precambrian samples, 340 Myr for the Cambrian samples and 130 Myr for the Lower Cretaceous samples – according to burial times (see text for justification).

a.

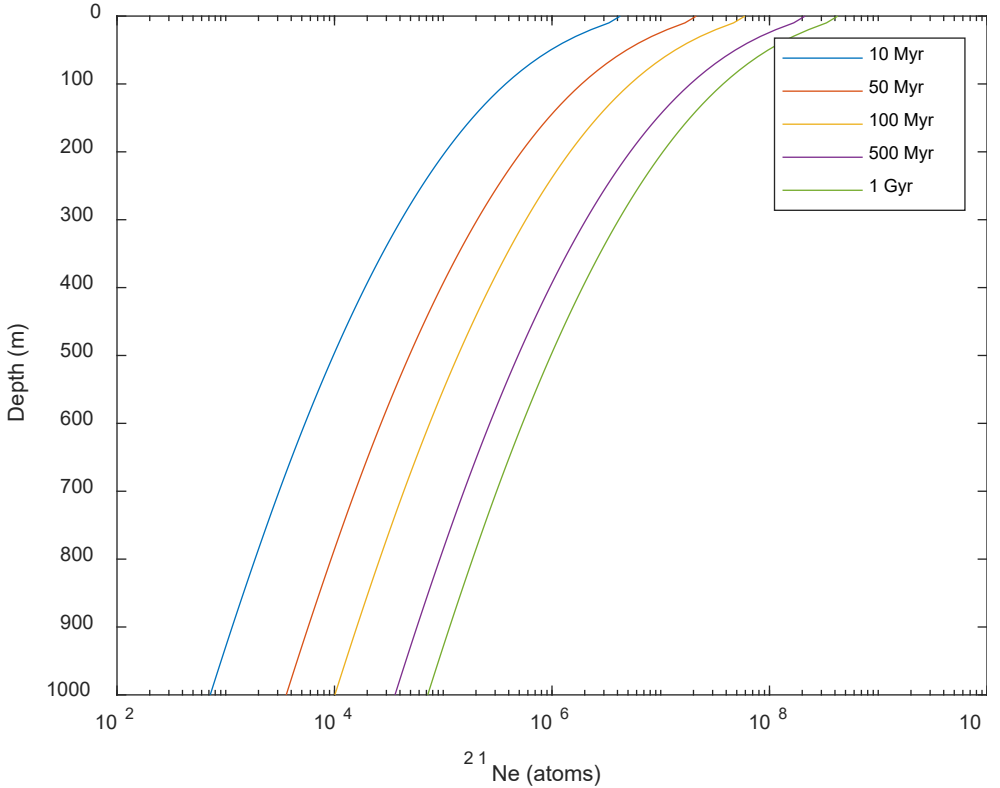
0
100
200
300
400
500
600
700
800
900
1000
Depth (m)
10 2
10 4
10 6
10 8
10
21Ne (atoms)
10 Myr
50 Myr
100 Myr
500 Myr
1 Gyr

b.

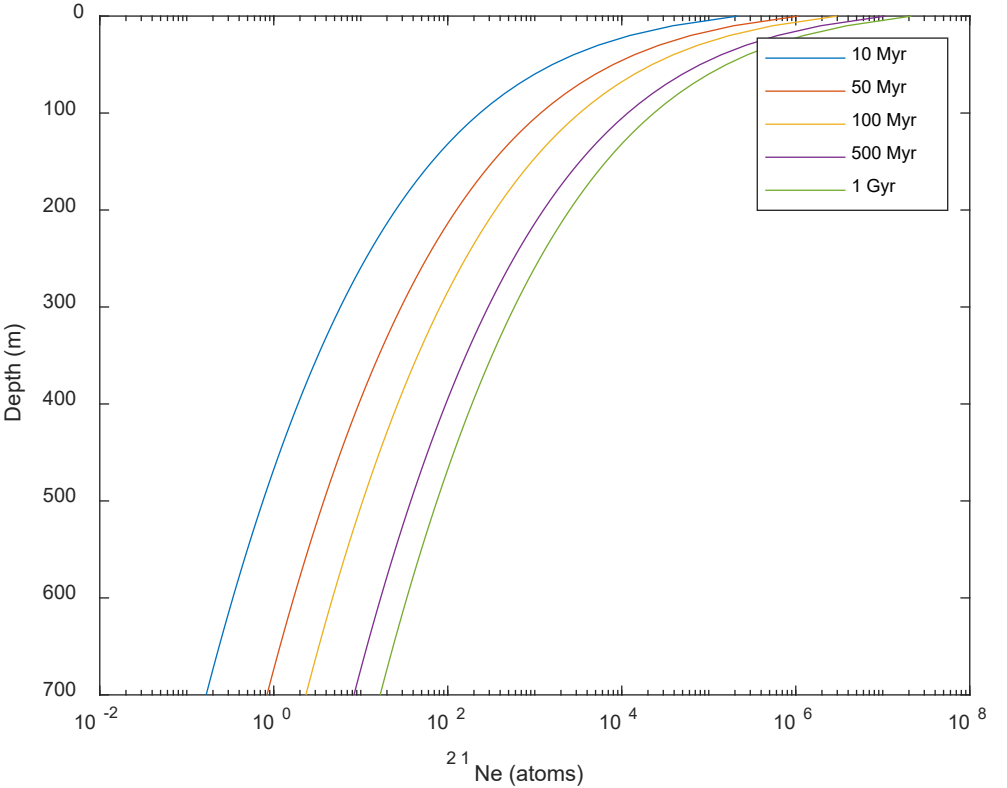
0
100
200
300
400
500
600
700
Depth (m)
10 -2
10 0
10 2
10 4
10 6
10 8
21Ne (atoms)
10 Myr
50 Myr
100 Myr
500 Myr
1 Gyr

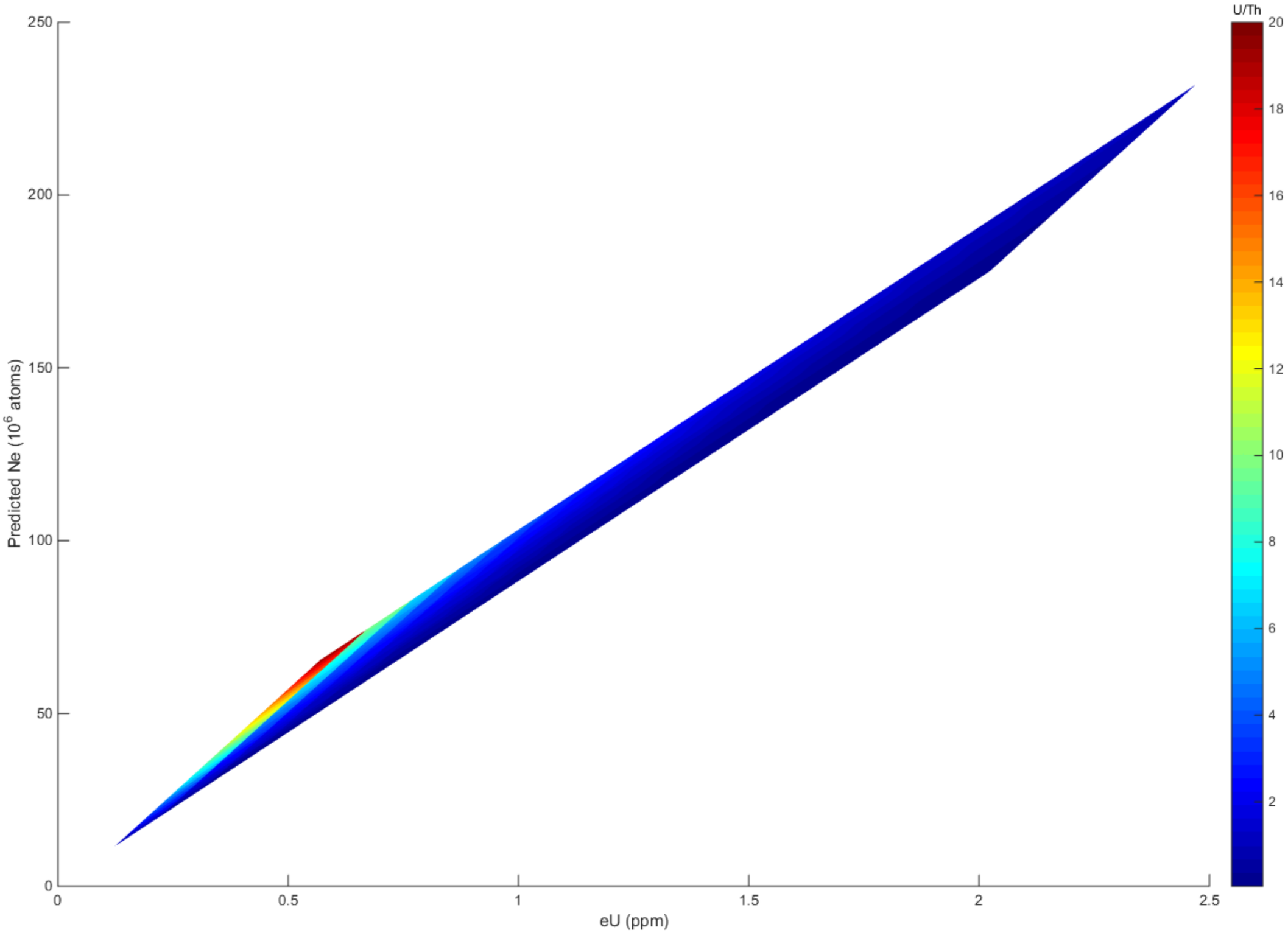
Predicted Ne (10^6 atoms)
250
200
150
100
50
0
0
0.5
1
1.5
2
2.5
eU (ppm)
U/Th
20
18
16
14
12
10
8
6
4
2

a.

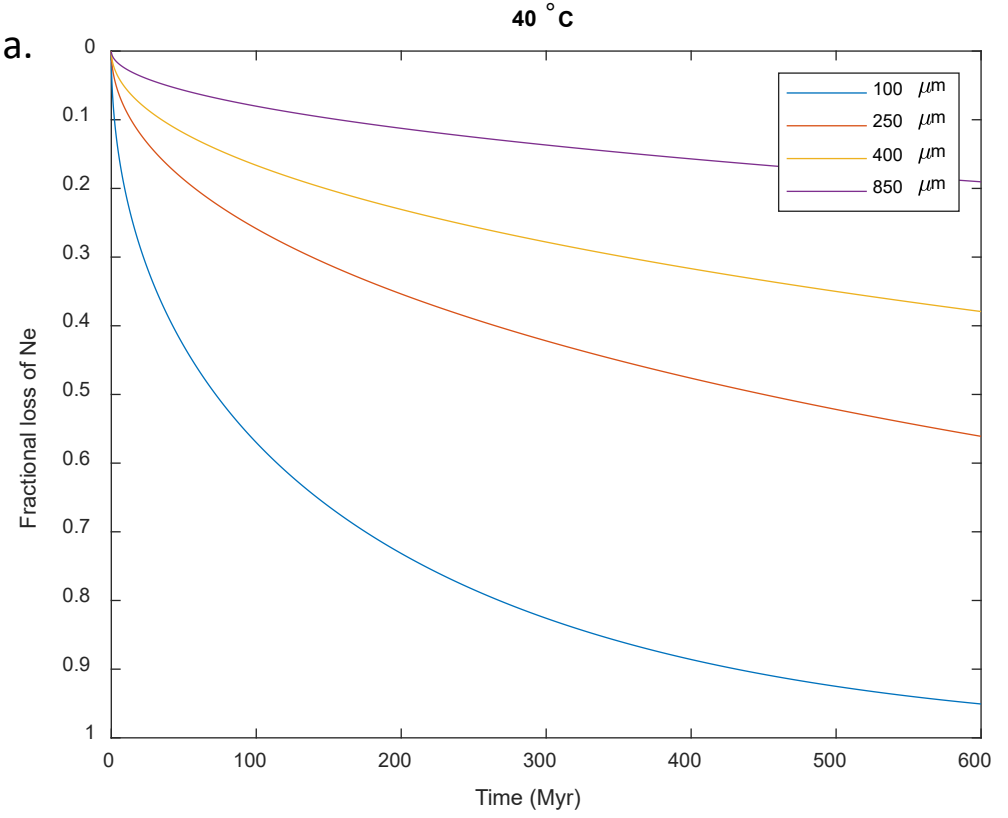
40 °C
Fractional loss of Ne
Time (Myr)
100 μm
250 μm
400 μm
850 μm
0
0.1
0.2
0.3
0.4
0.5
0.6
0.7
0.8
0.9
1
0
100
200
300
400
500
600

b.

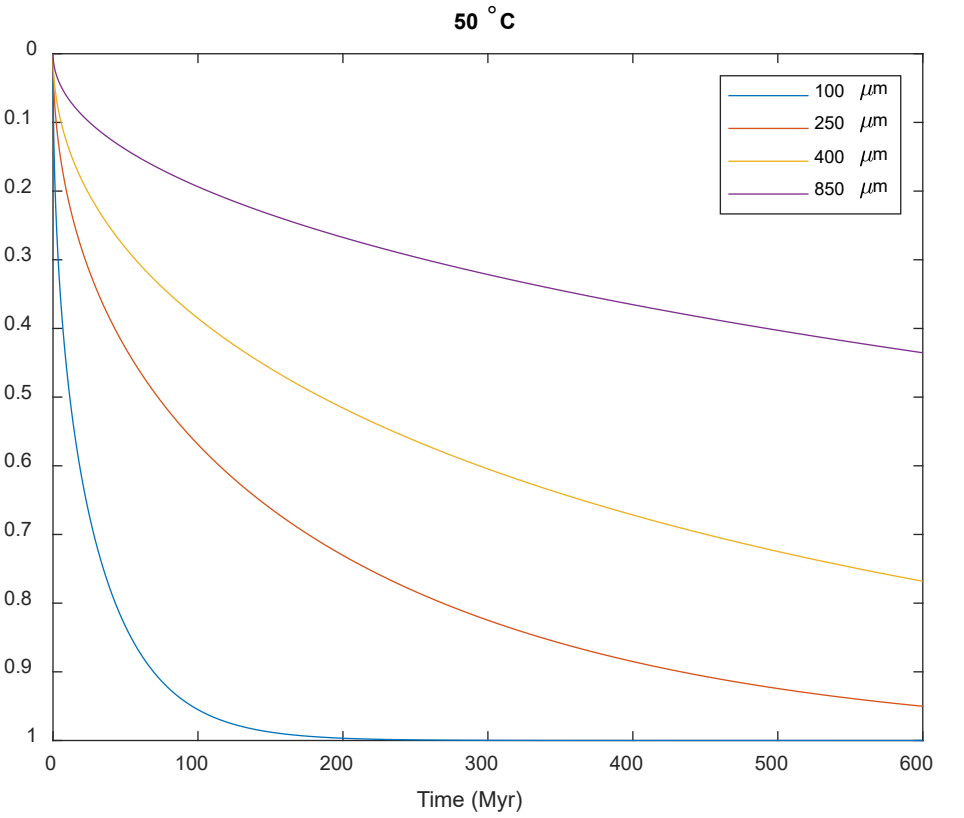
50 °C
Time (Myr)
100 μm
250 μm
400 μm
850 μm
0
0.1
0.2
0.3
0.4
0.5
0.6
0.7
0.8
0.9
1
0
100
200
300
400
500
600

c.

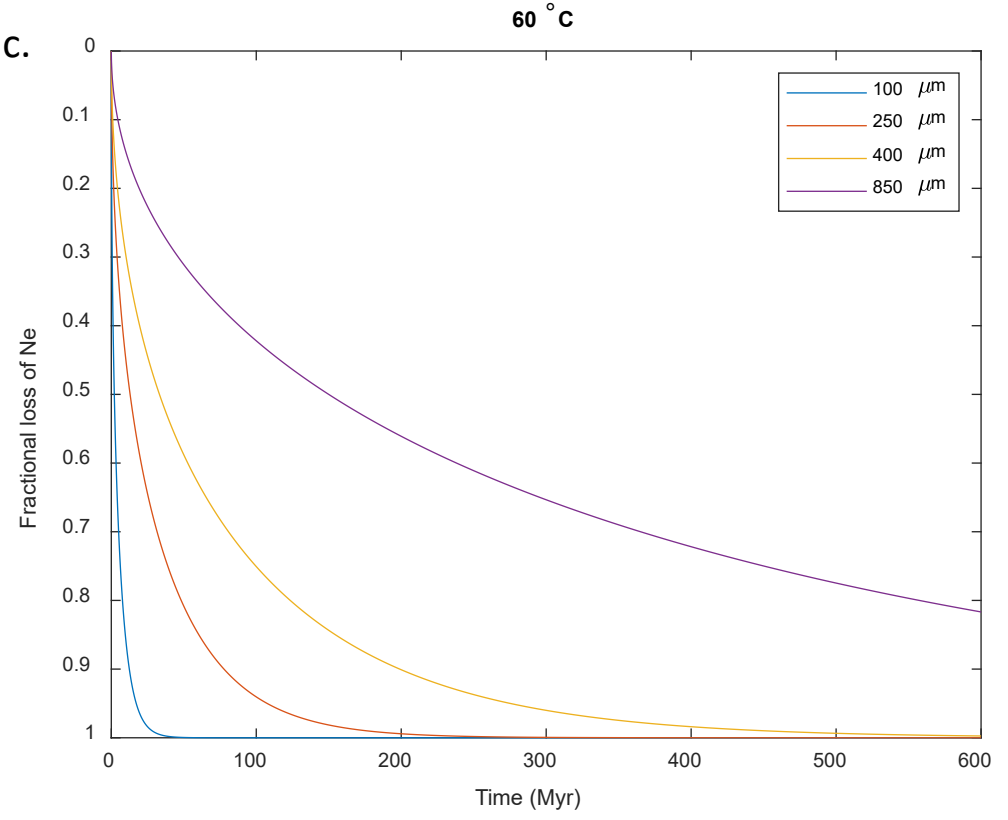
60 °C
Fractional loss of Ne
Time (Myr)
100 μm
250 μm
400 μm
850 μm
0
0.1
0.2
0.3
0.4
0.5
0.6
0.7
0.8
0.9
1
0
100
200
300
400
500
600

a.

34°E
35°E
36°E
33°N
32°N
31°N
30°N
29°N
Mt. Ramim
Jericho
Ramon
Sinaf
N
0 25 50 100
Kilometers

b.

Proto -
Tethys
Ocean
Minoan terranes
Cadomian terranes
Avalonian terranes
East Gondwana
West Gondwana
Sahara Meta Craton
Arabian-Nubian Shield
West Africa
Congo
India
Ama-zonia
Sao Franc.
Australia
Baltica
Rio de la Plata
Kalahari
Antarctica
North America
Precambrian shield (Archean and Paleoproterozoic)
Neoproterozoic mobile belts
Neoproterozoic juvinile crust of Arabian-Nubian Shield
Mezoproterozoic and Grenvillian/Kibarab mobile belts

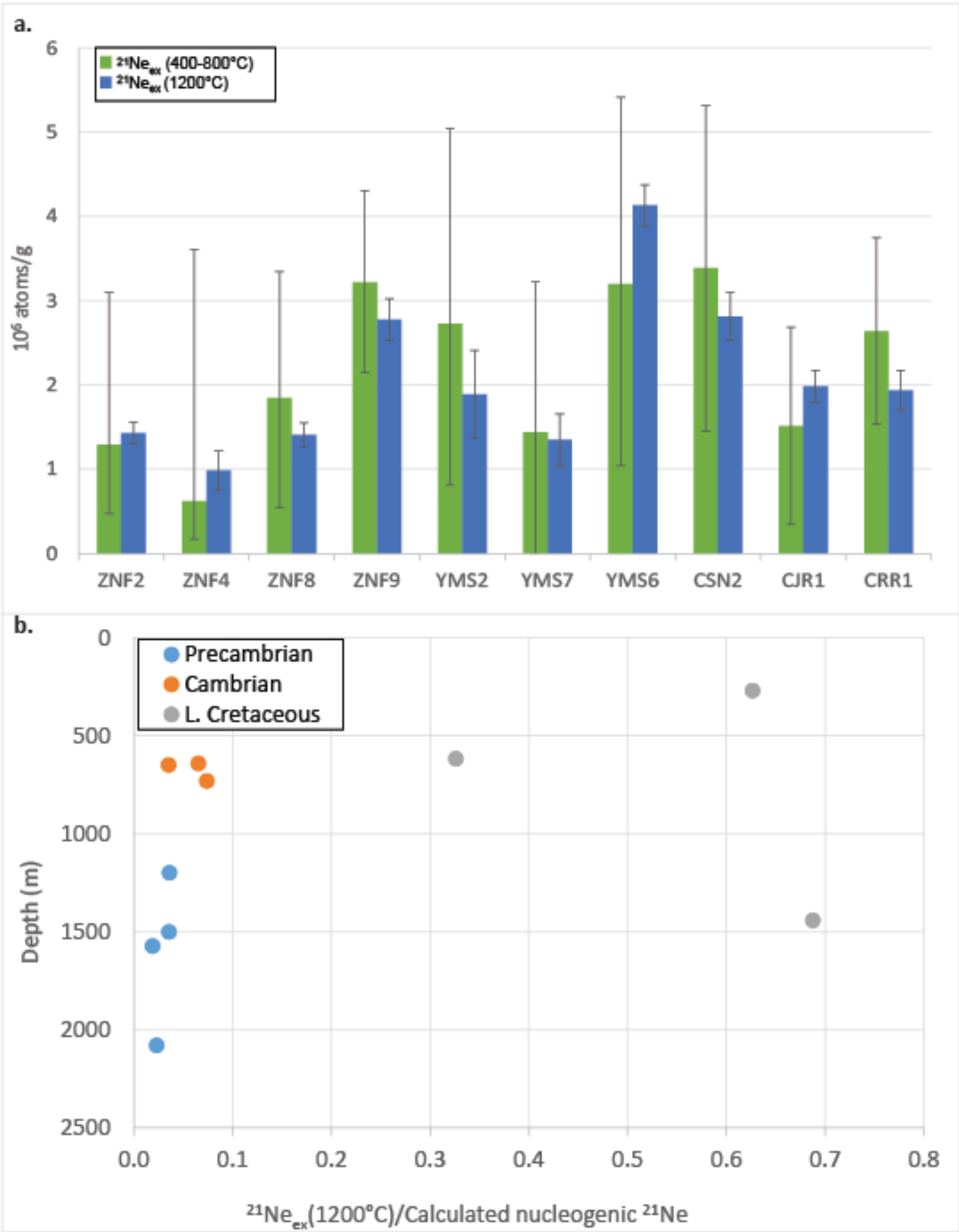
a.
$^{21}Ne_{ex}$ (400-800°C)
$^{21}Ne_{ex}$ (1200°C)
10^6 atoms/g
0
1
2
3
4
5
6
ZNF2
ZNF4
ZNF8
ZNF9
YMS2
YMS7
YMS6
CSN2
CJR1
CRR1
b.
Precambrian
Cambrian
L. Cretaceous
Depth (m)
0
500
1000
1500
2000
2500
0.0
0.1
0.2
0.3
0.4
0.5
0.6
0.7
0.8
$^{21}Ne_{ex}$(1200°C)/Calculated nucleogenic ^{21}Ne

Table 1
Information on samples and sampling locations

Sample	Sampling Site[a]	Era	Formation	Depth[b] (m)
CSN2	Sinaf01	Lower Cretaceous	Lower Amir	590
CJR1	Jericho01	Lower Cretaceous	Zewiera	1441
CRR1	Mt. Ramim	Lower Cretaceous	Zewiera	268
YMS02	Sinaf01	Cambrian	Shehoret	648
YMS07	Sinaf01	Cambrian	Shehoret	640
YMS06	Sinaf01	Cambrian	Amudei Shelomo	730
ZNF02	Sinaf01	Precambrian	Zenifim	1198
ZNF04	Sinaf01	Precambrian	Zenifim	1500
ZNF08	Ramon	Precambrian	Zenifim	2079
ZNF09	Ramon	Precambrian	Zenifim	1572

[a] All samples were taken from borehole material kept at the Geological Survey of Israel core repository.
[b] Depth is measured from the top of the core drilled (Fleischer and Varsahvsky, 2002).

Table 2.
Results of Ne analyses of quartz separates from samples from Precambrian, Cambrian, and Lower Cretaceous sediments

Sample	T (°C)	^{20}Ne (10^{-12} cm^3/g)	±	$^{22}Ne/^{20}Ne$	±	$^{21}Ne/^{20}Ne$	±
ZNF1-3	Crushed	737	40	0.10128	0.00028	0.002959	0.000046
ZNF4	Crushed	658	34	0.10175	0.00025	0.002972	0.000045
YMS4	Crushed	2150	110	0.10172	0.00026	0.002964	0.000037
YMS5	Crushed	861	44	0.1015	0.0014	0.002993	0.000039
CSN1	Crushed	443	27	0.10222	0.00050	0.002939	0.000048
CJR1	Crushed	663	35	0.10213	0.00032	0.002947	0.000044
CRR1	Crushed	322	23	0.10243	0.00046	0.002960	0.000063
CSN1	400°C	188	14	0.1025	0.0014	0.003003	0.000066
	600°C	882	63	0.10179	0.00053	0.003021	0.000044
	800°C	427	31	0.10255	0.00060	0.003037	0.000081
	1200°C	17.7	1.5	0.1054	0.0023	0.00886	0.00046
CJR1	400°C	221	16	0.10234	0.00090	0.002956	0.000095
	600°C	414	29	0.10179	0.00031	0.002994	0.000046
	800°C	213	15	0.10244	0.00046	0.00311	0.00011
	1200°C	10.0	1.0	0.1041	0.0041	0.01035	0.00057
CRR1	400°C	3.1	0.4	0.088	0.010	0.00309	0.00059
	600°C	361	22	0.10268	0.00099	0.003114	0.000065
	800°C	218	14	0.10268	0.00058	0.003153	0.000095
	1200°C	6.2	0.8	0.1111	0.0071	0.0146	0.0016
YMS2	400°C	103.4	5.3	0.1019	0.0012	0.00299	0.00016
	600°C	888	45	0.10136	0.00041	0.003005	0.000054
	800°C	1125	57	0.10118	0.00029	0.003021	0.000040
	1200°C	223	11	0.10270	0.00015	0.003281	0.000077
YMS6	400°C	74.1	4.0	0.1016	0.0013	0.00304	0.00013
	600°C	937	49	0.10114	0.00032	0.003058	0.000048
	800°C	1133	59	0.10181	0.00027	0.003052	0.000032
	1200°C	49.3	2.7	0.1049	0.0019	0.006117	0.000099
YMS7	400°C	135.3	8.5	0.1012	0.0020	0.00296	0.00015
	600°C	389	24	0.1017	0.0010	0.003060	0.000097
	800°C	524	32	0.10216	0.00089	0.002995	0.000085
	1200°C	82.6	5.1	0.10409	0.00071	0.00357	0.00013
ZNF2	400°C	354	19	0.10186	0.00069	0.002977	0.000049
	600°C	524	29	0.10148	0.00061	0.002991	0.000075
	800°C	469	26	0.10159	0.00021	0.003010	0.000080
	1200°C	17.1	1.2	0.1041	0.0024	0.00607	0.00030
ZNF4	400°C	830	42	0.10121	0.00050	0.002960	0.000043
	600°C	782	40	0.10125	0.00027	0.002984	0.000068
	800°C	1138	58	0.10183	0.00026	0.002983	0.000054
	1200°C	73.1	3.8	0.10439	0.00097	0.00347	0.00011
ZNF8	400°C	163.7	8.4	0.1017	0.0014	0.003062	0.000046
	600°C	329	17	0.10107	0.00060	0.003171	0.000072
	800°C	279	14	0.10088	0.00038	0.003196	0.000076
	1200°C	26.0	1.5	0.1025	0.0025	0.00508	0.00016
ZNF9	400°C	52.5	2.8	0.1019	0.0013	0.002979	0.000170
	600°C	419	21	0.10121	0.00044	0.003225	0.000059
	800°C	283	14	0.10118	0.00095	0.003257	0.000077
	1200°C	10.3	0.9	0.1057	0.0027	0.0131	0.0011

For samples ZNF2 and ZNF4 the crusher aliquot used for $^{21}Ne_{ex}$ calculations is ZNF1-3, for sample ZNF9 crusher aliquot used is ZNF8, for sample YMS2 crusher aliquot used is YMS4 and for sample YMS6 crusher aliquot used is YMS5. All measurement uncertainties are 2σ.

Table 3

Comparison between measured and calculated nucleogenic ^{21}Ne and loss by diffusion compared to nucleogenic Ne retention

Sample	Depth	U[a]	Th[a]	$^{21}Ne_{ex}$ 400-800°C	$^{21}Ne_{ex}$ 1200°c	Calculated nucleogenic ^{21}Ne[b]	Fraction loss from diffusion[c]			$^{21}Ne_{nucleogenic}$ measured/calculated
	(m)	(ppb)	(ppb)	(10^6 at/g)	(10^6 at/g)	(10^6 at/g)	250µm	850µm	Mean	
CSN01	590	593	154	3.4±1.9	2.81±0.29	11	0.23	0.07	0.12	0.33
CJR01	1441	484	106	1.5±1.2	1.98±0.19	9	0.78	0.30	0.47	0.69
CRR01	269	333	107	2.6±1.1	1.94±0.24	6	0.12	0.04	0.06	0.63
YMS02	648	552	1153	$2.7^{+2.3}_{-1.9}$	1.89±0.52	42	0.42	0.14	0.23	0.04
YMS07	640	212	414	$1.4^{+1.8}_{-1.1}$	1.35±0.31	21	0.42	0.13	0.22	0.07
YMS06	730	492	1430	3.2±2.2	4.13±0.25	44	0.48	0.16	0.25	0.07
ZNF02	1198	275	643	$1.3^{+1.8}_{-0.8}$	1.43±0.13	40	0.92	0.40	0.60	0.04
ZNF04	1500	224	353	$0.6^{+3.0}_{-0.4}$	0.98±0.23	68	1.00	0.61	0.82	0.04
ZNF08	2079	476	838	$1.8^{+1.5}_{-1.3}$	1.41±0.14	21	1.00	0.98	1.00	0.02
ZNF09	1572	877	2780	3.2±1.1	2.77±0.25	147	1.00	0.67	0.86	0.02

[a] Measurement uncertainties for U and Th are ~5%.

[b] Uncertainties for nucleogenic Ne calculations are not presented due to unknown random errors.

[c] Diffusion is calculated using a normal geothermal gradient of 20 K/km and 25°C at the surface and given depths for all samples. The calculated uncertainties based on the kinetic coefficient uncertainties reported by Tremblay et al. (2014a) add up to ~2%. The actual uncertainties for these calculations correspond to burial depth and grain size and are largely unknown.